

Metamaterials and plasmonics: From nanoparticles to nanoantenna arrays, metasurfaces, and metamaterials

This content has been downloaded from IOPscience. Please scroll down to see the full text.

2014 Chinese Phys. B 23 047809

(<http://iopscience.iop.org/1674-1056/23/4/047809>)

View [the table of contents for this issue](#), or go to the [journal homepage](#) for more

Download details:

IP Address: 141.215.185.76

This content was downloaded on 04/10/2016 at 21:42

Please note that [terms and conditions apply](#).

You may also be interested in:

[Plasmonic nanoparticles: Towards the fabrication of biosensors](#)

Hui Shen

[Recent advances on optical metasurfaces](#)

Yang Zhao, Xing-Xiang Liu and Andrea Alù

[Theory of a double-quantum-dot spaser](#)

E S Andrianov, A A Pukhov, A V Dorofeenko et al.

[Superresolution and enhancement in metamaterials](#)

Andrei N Lagarkov, Andrei K Sarychev, V N Kissel et al.

[Longitudinal polarizability and enhancement factor of a tapered optical gold nanoantenna](#)

A R Gazizov, S S Kharintsev and M Kh Salakhov

[L-shaped metasurface for both linear and circular polarization conversions](#)

Wei Wang, Zhongyi Guo, Rongzhen Li et al.

[Design and Numerical Analyses of Ultrathin Plasmonic Lens for Subwavelength Focusing by Phase Discontinuities of Nanoantenna Arrays](#)

Jing Lin, Shibin Wu, Xiong Li et al.

Metamaterials and plasmonics: From nanoparticles to nanoantenna arrays, metasurfaces, and metamaterials*

Francesco Monticone and Andrea Alù[†]

Department of Electrical and Computer Engineering, The University of Texas at Austin, 1 University Station C0803, Austin, Texas 78712, USA

(Received 8 January 2014; revised manuscript received 29 January 2014; published online 20 March 2014)

The rise of plasmonic metamaterials in recent years has unveiled the possibility of revolutionizing the entire field of optics and photonics, challenging well-established technological limitations and paving the way to innovations at an unprecedented level. To capitalize the disruptive potential of this rising field of science and technology, it is important to be able to combine the richness of optical phenomena enabled by nanoplasmonics in order to realize metamaterial components, devices, and systems of increasing complexity. Here, we review a few recent research directions in the field of plasmonic metamaterials, which may foster further advancements in this research area. We will discuss the anomalous scattering features enabled by plasmonic nanoparticles and nanoclusters, and show how they may represent the fundamental building blocks of complex nanophotonic architectures. Building on these concepts, advanced components can be designed and operated, such as optical nanoantennas and nanoantenna arrays, which, in turn, may be at the basis of metasurface devices and complex systems. Following this path, from basic phenomena to advanced functionalities, the field of plasmonic metamaterials offers the promise of an important scientific and technological impact, with applications spanning from medical diagnostics to clean energy and information processing.

Keywords: plasmonics, metamaterials, nanoparticles, scattering

PACS: 78.67.Pt, 73.20.Mf, 78.67.Bf, 42.25.Fx

DOI: 10.1088/1674-1056/23/4/047809

1. Introduction

The field of metamaterials has become today a multidisciplinary enterprise, encompassing applied physics, engineering, material science, and nanotechnology, aimed at designing materials with physical properties beyond those readily available in nature.^[1] Such emphasis in going “beyond” (“meta” in Greek) natural materials has been the driving force in this area, which, in the last ten years, building on earlier findings on complex media,^[2,3] has allowed challenging and overcoming physical limitations that seemed written in stone for decades and, in a few cases, even centuries. Notable examples include the experimental demonstration of negative index of refraction,^[4] which was generally thought to be impossible at the time of the seminal theoretical paper by Veselago in 1967,^[5] marking the tipping point for the field of electromagnetic metamaterials. Negative refraction is also at the basis of perfect lensing^[6] that, relying on the amplification of the evanescent portion of the impinging fields, in principle allows beating the diffraction limit discovered by Abbe in 1837.^[7] In their short history, metamaterials have been applied to the most diverse areas, including invisibility cloaks,^[8–13] artificial optical black holes,^[14,15] cosmology,^[16] high-temperature superconductors,^[17] just to name a few particularly fascinating examples.

Metamaterials owe their fascinating properties to the

careful engineering of their underlying structure, or meta-atoms. As a result, metamaterials are not simply mixtures of different materials and, by their same definition, a metamaterial composed of two constituent materials is required to have electromagnetic properties drastically different from both constituents. Although several accepted definitions of metamaterials^[3] emphasize the importance of the structure in determining the emerging electromagnetic properties, this aspect, without further clarifications, is somewhat ambiguous, as it applies, for instance, also to photonic crystals.^[18] Photonic crystals, however, derive their anomalous properties from higher-order spatial modes, whereas metamaterials work with the dominant propagation mode, and can be described as a continuum, supported by an arrangement of subwavelength inclusions with subwavelength spacing between neighboring elements. The macroscopic effective properties of metamaterials can then be obtained by applying several mixing rules^[19,20] and homogenization principles.^[21] In order to realize interesting and anomalous electromagnetic properties, it is necessary to rely on a strong interaction of the impinging radiation with the meta-atoms, which is typically obtained when the inclusions are close to a resonance. Given their subwavelength size, however, dielectric meta-atoms are typically largely off-resonance, meaning that the impinging harmonic electric field and the induced dipole moment of the small in-

*Project supported by the ONR MURI (Grant No. N00014-10-1-0942).

[†]Corresponding author. E-mail: alu@mail.utexas.edu

clusions oscillate almost in-phase and thereby small energy can be extracted from the impinging field to interact with the material. Plasmonics offers an ideal solution to this problem at optical frequencies, as the impinging photons can couple with collective oscillations of the electron gas in metals, called plasmons, and the resulting “plasmon polaritons” determine very strong, highly confined light-matter interactions, field enhancement, and confinement over deeply subwavelength volumes and largely reduced resonance lengths.^[22] As an example, the prehistory of optical metamaterials may be traced back to the plasmonic resonances of colloidal nanoparticles at the basis of the bright colors of the Gothic cathedral’s stained glasses, whose optical properties (their color) are very different from the properties of the material constituents (gold nanoparticles, for example, determine a bright red color).

In analogy with the microelectronics revolution of the past decades, for metamaterials to make a true technological impact, it is necessary to move upward in the “design stack”, from the physical layer dealing with materials and basic phenomena, to the device and system layers, enabling advanced functionalities by suitably combining the basic effects at an architecture level. Within this context, we will present and outline in this review paper a few particularly exciting research directions that have recently come to prominence in the field of plasmonic metamaterials and hold the potential to further push the boundaries of this research area at different levels of the design stack. In Section 2, we will discuss several anomalous scattering effects enabled by plasmonics, such as plasmonic resonances in nanoparticles and nanoclusters, scattering-cancellation cloaking, and plasmonic Fano resonances. In Section 3, the recently introduced paradigm of optical nanocircuits will be presented, which allows parameterizing and modularizing the optical response in terms of basic “lumped” building blocks. The anomalous scattering effects presented in Section 2 will be discussed within this framework, which is also instrumental in the design, tuning, and matching of optical nanoantennas. Finally, with this toolbox of concepts, in Section 4 we will present the latest progress in optical metasurfaces — the planarized version of metamaterials — which may have the disruptive potential to advance the entire field of nano-optics at the device and system levels, by practically realizing many of the functionalities enabled by three-dimensional (3D) metamaterials, while relaxing their inherent challenges and limitations, and potentially introducing tunable and reconfigurable capabilities.

2. Anomalous scattering effects in plasmonic nanoparticles and nanoclusters

Electromagnetic wave interaction with a spherical material object can be exactly computed by applying the rigorous

Mie scattering theory.^[23] Impinging and scattered fields, as well as the total fields inside the object, may be written as the superposition of transverse-electric (TE) and transverse-magnetic (TM) spherical harmonics, in a spherical coordinate system centered with the object. By applying proper electromagnetic boundary conditions at the spherical interfaces, the complex weight coefficients of the spherical harmonics can be found, which uniquely determine the fields everywhere. In particular, the scattering coefficients can be conveniently written as

$$c_n = -\frac{U_n}{U_n + iV_n}, \quad (1)$$

where we assumed an $e^{-i\omega t}$ time convention and the quantities U_n, V_n are obtained by solving appropriate determinants associated with the boundary conditions for the geometry under consideration.^[24] The n -th scattering coefficient quantifies the coupling of the impinging energy into the n -th multipolar scattering/radiation channel; for example, the first TM scattering coefficient c_1^{TM} corresponds to the electric dipole moment contribution, which is of particular interest, as it dominates the scattering in the quasi-static regime, namely, when the sphere is small compared to the impinging wavelength. Scattering resonances occur when $|c_n| = 1$, indicating that maximum power is coupled into the n -th scattering channel. This condition is met when $V_n = 0$, which, for a homogenous and isotropic sphere, becomes

$$j_n(x) [x_0 y_n(x_0)]' = y_n(x_0) [x j_n(x)]' / \epsilon \quad (2)$$

for TM spherical harmonics (the TE case is obtained by duality). $j_n(\cdot)$ and $y_n(\cdot)$ are the spherical Bessel and Neumann functions of order n , respectively; $x_0 = a\omega\sqrt{\epsilon_0\mu_0}$ and $x = x_0\sqrt{\epsilon\mu}$, where ω is the angular frequency, ϵ_0 and μ_0 are the free-space permittivity and permeability, a is the radius of the sphere and ϵ and μ its relative permittivity and permeability. The prime symbol indicates derivative with respect to the argument.

When the entire denominator of Eq. (1) vanishes, the scattering coefficient goes to infinity, which corresponds to a “scattering pole” (Fig. 1(a)). Passivity requires the frequency at which a scattering pole occurs to be complex ($\omega = \omega_r + i\omega_i$), since power conservation implies that $|c_n|$ is bounded between 0 and 1 on the real frequency axis. Besides, scattering poles are restricted to the lower half of the complex frequency plane, i.e., $\omega_i < 0$, due to causality (the time response of the system must be zero for negative time instants). The scattering poles correspond to the natural eigenmodes of the scattering system and their eigenfrequencies can be obtained by solving the transcendental equation $U_n + iV_n = 0$, which, for the same isotropic and homogeneous sphere, takes the form

$$j_n(x) [x_0 h_n^{(1)}(x_0)]' = h_n^{(1)}(x_0) [x j_n(x)]' / \epsilon \quad (3)$$

for TM spherical harmonics (again, the TE case may be obtained by duality). $h_n^{(1)}(\cdot) = j_n(\cdot) + i y_n(\cdot)$ is the spherical Hankel function of first kind. The imaginary part of the complex eigenfrequencies, solution of Eq. (3), is related to the damping of the corresponding eigenmode oscillation (in the lossless case, the radiation damping). If this imaginary part is small, the real part of the eigenfrequency is generally close to the real frequency of a corresponding scattering resonance solution of Eq. (2).

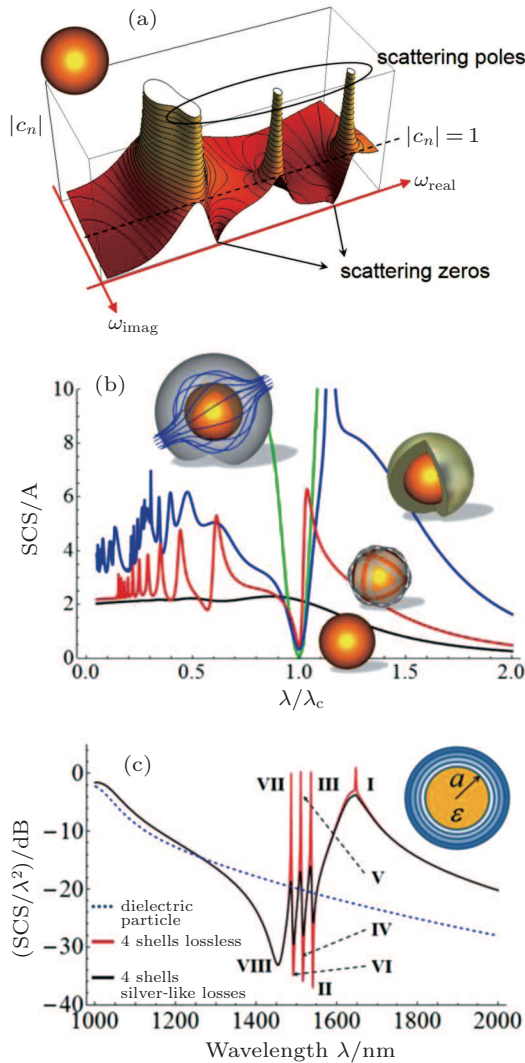


Fig. 1. Nanoparticles for resonant scattering, cloaking, and Fano resonances. (a) Typical appearance of the scattering coefficients on the complex frequency plane, for a homogenous sphere. Scattering zeros and poles are indicated. Scattering resonances occur when the scattering coefficient reaches one on the real frequency axis (dashed line). By using composite plasmonic nanoparticles, e.g., core-shell spheres, it is possible to control the zero-pole pattern to a large extent. (b) Scattering cross section for plasmonic cloaking (blue curve), transformation-optics (green), and mantle cloaking (red), showing increased overall scattering over the entire spectrum compared to the uncoated particle (black curve) (from Ref. [34]). (c) Multilayered plasmonic particle supporting a peculiar comb-like scattering spectrum, characterized by multiple closely-spaced Fano resonances (from Ref. [40], Fig. 1).

For a dielectric sphere, the first scattering resonance occurs when the incident wavelength is comparable to the di-

mension of the sphere and the scattering poles are associated with the natural modes of the open dielectric cavity. Resonant scattering for deeply subwavelength particles requires, instead, either large values of the dielectric constant, or plasmonic materials with small negative real part of permittivity. Notably, for the spherical geometry in quasi-static regime, a plasmonic resonance occurs when the well-known condition $\text{Re}[\epsilon(\omega_0)] \approx -2$ is met.^[22] At the frequency ω_0 , the localized surface plasmon resonates under the harmonic excitation of the impinging wave, resulting in strongly enhanced fields, localized in deeply subwavelength volumes much below the diffraction limit, accompanied by resonant scattering and large absorption. These properties are ideal for applications that may benefit from high local fields, such as for sensing and imaging,^[25,26] light harvesting,^[27] photovoltaics (particularly thin-film, and organic solar cells),^[28] surface-enhanced fluorescence and Raman scattering,^[29] enhanced nonlinear response for harmonic generation and optical bistability.^[30] The dispersion of the plasmonic material, the shape of the particles and the combination with other materials are all factors that allow engineering the resonant frequency ω_0 to a large extent, for applications in different spectral ranges.

Borrowing terminology from electrical and systems engineering, the scattering poles on the complex frequency plane are accompanied by “scattering zeros” (Fig. 1(a)), whose position, however, is not restricted by causality, and passivity. When a zero of the n -th scattering coefficient occurs on the real frequency axis, an incident field oscillating at that frequency does not induce any scattering for the n -th spherical order (although it may induce currents inside the object). These concepts are at the basis of scattering-cancellation cloaking techniques, such as plasmonic cloaking^[8] or mantle cloaking.^[12] With these cloaking schemes, transparency, or invisibility, is obtained by inducing a “secondary” scattered field that counteracts and cancels the scattering from the object to be concealed. To achieve this goal, plasmonic cloaking relies on the local negative polarizability of plasmonic shells, whereas mantle cloaking is based on specific current patterns induced on suitably tailored metasurface cloaks. More in general, the ultimate goal of an invisibility cloak is to place scattering zeros in the desired location on the complex frequency plane, such that the desired invisibility performance is obtained. Interestingly, the requirements on the scattering zeros do not imply the fields to vanish inside the original object, instead, the internal fields may be large, a characteristic feature of scattering-cancellation schemes that may be exploited for low-invasive near-field sensing,^[31] such as for near-field scanning optical microscopy,^[32] or to realize all-optical switching.^[30] Besides, compared to other techniques, such as transformation-optics cloaking, scattering-cancellation schemes exhibit a larger bandwidth,^[33] due to

the non-resonant mechanism on which they are based. However, the performance of any cloak, in terms of bandwidth and scattering suppression, are subject to fundamental bounds ultimately deduced from the linearity, causality, and passivity of the scattering system. In other words, we cannot rearrange the scattering zero-pole pattern on the complex plane at will. In particular, whenever we introduce a passive cloak, we always replace free-space with matter, which responds to electromagnetic waves in a causal way. As recently demonstrated in Ref. [34], this fact implies that the total scattering cross section integrated over the entire electromagnetic spectrum always increases when we introduce a passive cloak, compared to the uncovered case. Except for a few interesting cases involving diamagnetic media and superconductors,^[34] a cloaked object actually scatters more over the whole spectrum than the bare object and, as a result, achieving ideal invisibility in a frequency range is always counterbalanced by much increased scattering in other regions of the spectrum (Fig. 1(b)). Such limitations of passive cloaks can be overcome with active cloaking schemes, which, by relying on external sources of energy, may exhibit much wider operational bandwidth. Recent examples include active arrays of antennas radiating fields that cancel the scattering from the object,^[35] or the use of operational amplifiers to realize mantle cloaks characterized by non-Foster reactance dispersion.^[36]

It is interesting to note that, in the conventional quasi-static approximation of the scattering coefficients (or the corresponding polarizabilities), the radiation damping is completely neglected, as discussed in Ref. [37]. As a result, the scattering poles given by Eq. (3), at which the scattering coefficients go to infinity, lie on the real frequency axis, evidently violating power conservation. Passivity is restored by properly introducing a radiation correction factor,^[37,38] which moves the poles back in the lower half of the complex frequency plane. Yet, if the electrical size of the object is small, the poles remain very close to the real frequency axis, and the real part of the eigenfrequencies is basically identical to the frequency of the scattering resonances at which the scattering coefficient is unitary. The proximity of the scattering poles to the real frequency axis, which indicates small radiation and ohmic damping, implies that scattering resonances and zeros almost strictly alternate as the real frequency increases,^[39,40] similar to the alternation of zeros and poles of a lossless dispersive impedance due to Foster's Reactance Theorem.^[41] Such alternation limits the achievable bandwidth for cloaking in the quasi-static regime, as it is not possible to have two cloaking frequencies without a scattering resonance between them. On the other hand, this fact can be exploited to our advantage to achieve some extreme scattering features. In fact, it has been shown in Ref. [40] that, based on this principle, a

multilayered plasmonic sphere can be designed such that scattering resonances and zeros are brought in close proximity on the real frequency axis, forming a "degenerate scattering state" at which the particle exhibits cloaking and resonance behaviors at arbitrarily close frequencies. This leads to extreme scattering signatures (Fig. 1(c)), including ultra-sharp dipole-dipole Fano resonances at optical^[30] and ultraviolet^[42] frequencies, comb-like scattering responses characterized by ideally strong super-scattering states closely coupled to invisible states,^[40] and electromagnetic-induced transparency features.^[43] The degeneracy between cloaking and resonant states has another interesting effect: at the cloaking frequency the scattering is very low, however, the close proximity with a scattering resonance leads to extremely high resonant fields inside the particle. Having a large and abrupt variation of scattering, from resonant to cloaking states, yet very large field intensity in both cases, is an ideal condition to exploit weak nonlinearities inside the particle to realize all-optical scattering switches and nanomemories.^[30]

The previous paragraphs discussed the anomalous scattering effects enabled by individual subwavelength plasmonic nanoparticles, stemming from the complex interplay of scattering zeros and poles of the dominant electric dipolar response. Even more interesting phenomena arise from properly engineered collections of closely spaced plasmonic nanoparticles, for which the plasmon modes of the different particles couple and interfere in the near-field, leading to collective plasmonic oscillations of the cluster, which support strong higher-order responses (e.g., magnetic dipole, electric quadrupole moments) at deeply subwavelength scales. Although plasmonic clusters can be rigorously studied with the generalized Mie theory,^[44] approximate techniques, such as the plasmon hybridization method,^[45,46] or analyses based on the dynamic dipolar interaction between nanoparticles,^[47] usually provide simple and intuitive physical insight, while capturing all the relevant phenomena. These methods, for example, can predict and explain the excitation of Fano resonances in plasmonic nanoclusters^[48] (Fig. 2(a)). Such resonances are interference phenomena arising in systems of coupled oscillators.^[49] In plasmonic clusters, they are usually determined by the interference of a broad electric dipolar resonance and a spectrally-overlapped narrower higher-order resonance, whose coupling is triggered by some form of symmetry breaking that changes the "selection rules" for mode interaction.^[48] The peculiar sharp and asymmetric lineshape of Fano resonances and the nature of their underlying interference mechanism make them very sensitive to small perturbations of the cluster geometry or modifications of the environment,^[50] a property that, combined with the high intensity of localized fields, is ideal to realize efficient sensing

platforms, for detection of chemicals and biological species, up to single molecular monolayers.^[51]

A notable example of nanoparticle cluster is the nanoring geometry shown in Fig. 2(b), which can sustain a resonant magnetic dipole collective response at optical frequencies, despite its overall subwavelength size and the purely electric response of the nanoparticles.^[47,52] In fact, despite the absence of natural magnetism at optical frequencies, it has been shown^[47,52,53] that a proper spatial dispersion of the permittivity profile may actually produce an effective magnetic response. Based on this principle, a collection of nanoparticles in a subwavelength ring configuration can be designed to exhibit a resonant magnetic response, sustained by a circulating displacement current guided by the plasmonic modes of the nanoparticles. In particular, a nanoring composed of N identical spheres resonates when

$$\text{Re} [\alpha_e^{-1}] = \sum_{j \neq j'}^{N-1} \text{Re} [G_{jj'}], \quad (4)$$

where α_e is the electric dipole polarizability of the nanopar-

ticles and $G_{jj'}$ are the Green's functions expressing the coupling between each pair of nanoparticles,^[47] fully considering retardation effects. Artificial optical magnetism produced by such subwavelength “meta-molecules” represents a viable solution to realize effective negative permeability and negative-index metamaterials at optical frequencies. Subsequent experimental attempts to verify these concepts,^[54] however, showed weak magnetic response, often hidden behind the much brighter electric dipole resonance, and substantially red-shifted due to the moderately large size of the cluster. Only recently, strong optical magnetism has been experimentally demonstrated based on subwavelength asymmetric nanorings.^[55] Thanks to the small size, in fact, magnetic and electric resonances are spectrally overlapped and, by suitably breaking the symmetry of the nanoring geometry, it is possible to trigger an interference between electric and magnetic plasmon modes, which induces a strong magneto–electric Fano resonance and efficiently boosts the optical magnetic response (Fig. 2(c)).

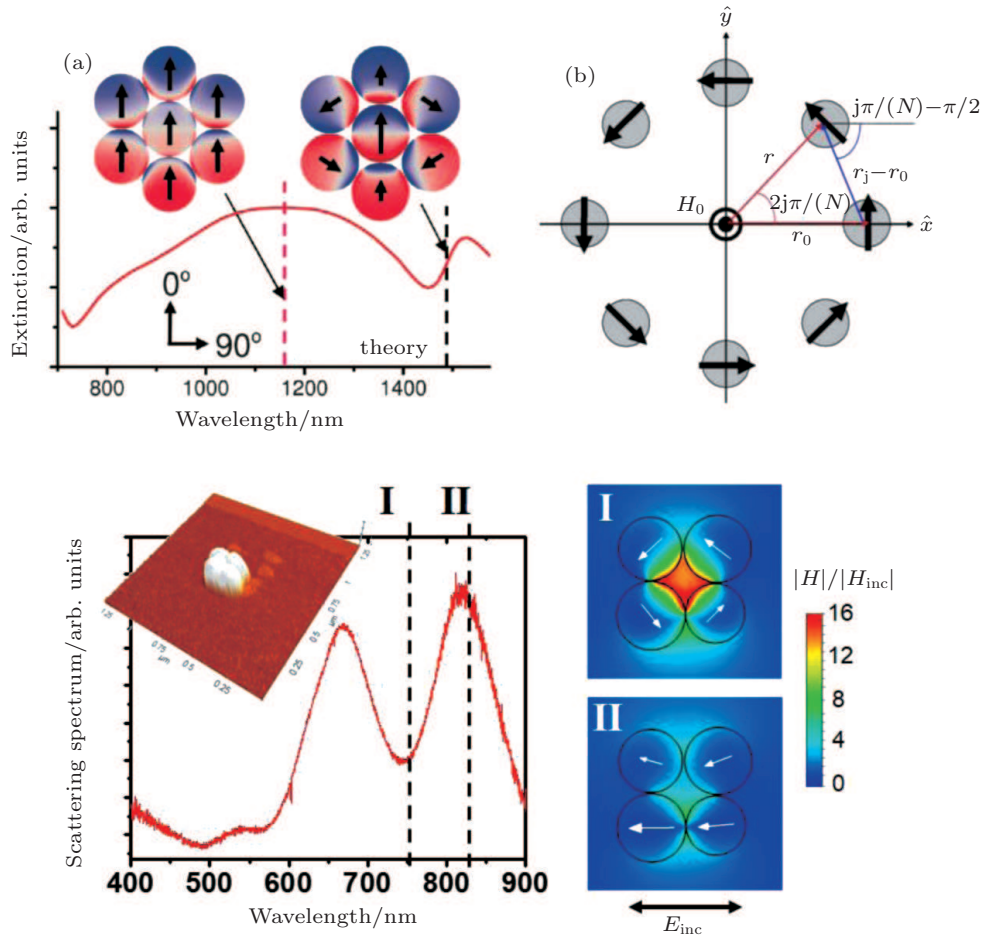


Fig. 2. Plasmonic nanoclusters and nanorings. (a) Calculated extinction spectrum of a plasmonic heptamer, with a marked asymmetric Fano resonance around 1450 nm. The insets show the charge distributions of the bright dipolar mode (left) and the dark mode (right) that induces the Fano resonance (from Ref. [54], Fig. 3(a)). (b) Symmetric ring of plasmonic nanoparticles, supporting resonant magnetic response at optical frequencies (from Ref. [47], Fig. 1). (c) Asymmetric nanoring (AFM image in the left inset) exhibiting a strong magneto–electric Fano resonance in the visible range and boosted optical magnetic response. The calculated field distributions on the right reveal a strong magnetic “hot spot” and circulating electric dipole moments at the Fano resonance dip around 750 nm (point I) (from Ref. [99]).

3. Modularizing the optical response of plasmonic nanoparticles: optical nanocircuits and nanoantennas

3.1. Optical nanocircuits

In Section 2, we discussed a few relevant examples of strong and peculiar light-matter interaction enabled by plasmonic structures, giving an idea of the richness of the optical response supported by plasmonic particles and clusters. The success of microelectronics in the last decades teaches us that, in order to take full advantage of this underlying physical richness, the complex response needs to be properly modularized in basic building blocks, which could then be combined to realize devices and systems of increasing complexity. In electronics, in fact, basic functionalities are synthesized by “lumped” circuit elements, such as resistors, inductors, capacitors, and transistors, and more complex operations are obtained by combining them in large circuits. The recently introduced paradigm of “metatronics” — metamaterial-inspired optical circuitry^[56,57] — aims at similarly modularizing the nanoscale optical response with “lumped optical nanocircuits”, providing the necessary concepts to move upward in the “design stack” from the level of nanoparticles and nanoclusters to more complex nanophotonic devices and systems.

At the basis of this modularization is the concept of optical impedance, which is defined, for a subwavelength nanoparticle, as the ratio of the local potential difference $V = |\mathbf{E}| l$ and the flux of displacement current $I_d = -i\omega\epsilon_0\epsilon |\mathbf{E}| S$ through the nanoparticle,^[58,59] where \mathbf{E} is the local electric field vector, l is the length of the nanoparticle along the electric field, S its transverse cross section and ϵ its relative dielectric constant. The optical impedance so defined is an intrinsic characteristic of the nanoparticle, independent of the surrounding environment, similar to its electrical counterpart. Based on this concept, a dielectric nanosphere of radius a corresponds to a nanocapacitance

$$C_{\text{sph}} = \pi a \epsilon_0 \text{Re}[\epsilon], \quad (5)$$

whereas a plasmonic nanosphere is modeled as a nanoinductance

$$L_{\text{sph}} = (-\omega^2 \pi a \epsilon_0 \text{Re}[\epsilon])^{-1}. \quad (6)$$

For a lossy particle, an equivalent nanoresistor is also added. The optical response of a subwavelength plasmonic nanosphere can then be quantitatively predicted by the simple nanocircuit model shown in Fig. 3(a) (right), composed of a nanoinductor representing the particle, connected in parallel with a nanocapacitor associated with the surrounding dipolar fringe fields ($C_{\text{fringe}} = 2\pi a \epsilon_0$), all driven by a current source

representing the applied field. The nanocircuit model correctly predicts the occurrence of a resonance for subwavelength plasmonic particles, as the nanoinductor resonates with the capacitive fringe fields; conversely, small dielectric particles cannot resonate due to their purely capacitive optical impedance.

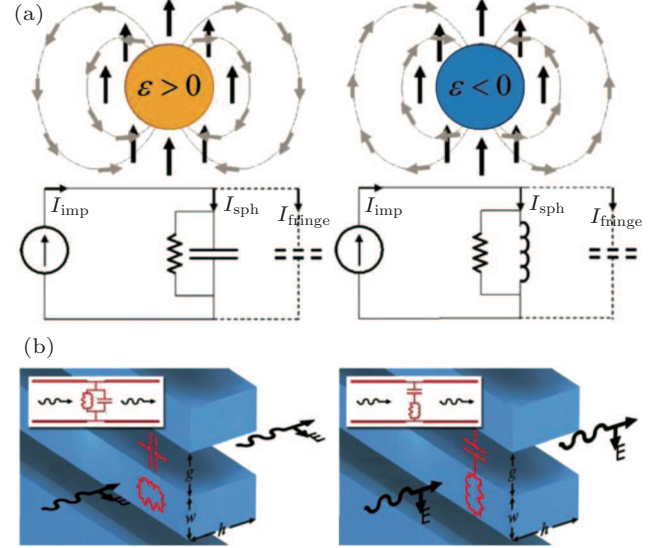


Fig. 3. Optical lumped nanocircuits. (a) Optical nanocircuit models of a dielectric (left) and a plasmonic nanoparticle (right). Black arrows denote the incident electric field, whereas grey arrows represent the electric dipolar fringe field from the nanospheres (from Ref. [58], Fig. 1). (b) Subwavelength grating of parallel plasmonic rods realizing a 2D optical nanocircuit with stereo-functionality, namely, the incident field polarization (or direction) selects the effective optical connection (series or parallel) between the nanoelements (from Ref. [61], Fig. 1).

Optical nanocircuits obey Kirchhoff’s circuit laws if retardation effects can be neglected (quasi-static regime), allowing to directly translate and transplant the simple and elegant design rules of electrical circuits to optical frequencies. Moreover, the interplay of scattering zeros and poles in plasmonic structures, which determines anomalous scattering effects as discussed in Section 2, finds a natural framework in the context of optical nanocircuits. Indeed, introducing new independent reactive elements in a circuit, such as new nanoparticles in a cluster or array, increases the order of the circuit and adds new complex zeros and/or poles to its response. By suitably designing the position of these zeros and poles on the complex frequency plane, following well-established design rules of electrical filters,^[60] it may be possible to implement advanced filtering functionalities at optical frequencies (e.g., Chebyshev or Butterworth filters^[60]) based on lumped nanocircuit elements.

Recent experiments^[61–63] have verified the validity and potential of the optical nanocircuit paradigm, also demonstrating the possibility of reconfiguring the circuit response by varying the incident direction and polarization, a useful feature not available with conventional electronic circuits. As shown in the 2D optical nanocircuit of Fig. 3(b), different incident

illuminations select different effective optical connections between the nanoelements of this “stereo-nanocircuit”, which may be exploited for parallel processing of multiple flows of information through a single nanostructure. Optical nanocircuit concepts have also been used in the design and tuning of optical nanoantennas^[63–65] and metasurfaces,^[66] as we will discuss in the following, and have provided useful physical insights to model several composite nanostructures, including circuit-based microcavity lasers,^[67] nanoparticle clusters, and nanorings,^[54,55] as well as to envision all-optical metamaterial circuit boards.^[68]

3.2. Optical nanoantennas

Recently, extensive research efforts have also been devoted to translate to optical frequency the concept of radio-frequency (RF) antennas, which has arguably been one of the key elements of the “information revolution” of the last century, allowing to enhance and control the energy transmitted and received in a wireless telecommunication system. In analogy with their RF counterparts, plasmonic optical antennas are defined as devices able to efficiently couple localized sources or guided waves at the nanoscale to far-field radiation and, by reciprocity, to convert the impinging radiation from the far-field into subwavelength localized or guided fields.^[69] Due to their plasmonic nature, however, optical nanoantennas exhibit novel and interesting phenomena not encountered at lower frequencies, making them an independent and exciting field of research. In fact, as frequency increases above the GHz range, into the THz region and beyond, the conduction properties of metals change dramatically, due to the finite electron density of states and their significant kinetic inductance that cause the electrons to respond to electromagnetic excitation with increasing phase lag, introducing a frequency-dispersive permittivity (typically Drude dispersion^[23]) with small negative real part, and associated plasmonic effects. As a result, the fields penetrate the plasmonic nanoantennas inducing a flow of displacement current $\mathbf{J}_d = -i\omega\mathbf{D} = -i\omega\epsilon_0\epsilon\mathbf{E}$, which, at sufficiently high frequency, becomes dominant over conduction effects. The plasmonic modes of the nanoantenna guide the oscillating displacement current, leading to extreme field enhancement and localization, which can be exploited to boost weak optical nonlinearities^[70–72] and enhance spontaneous emission from quantum dots and fluorescent molecules.^[73–75] More in general, a vast range of applications may largely benefit from the strong and peculiar light-matter interactions enabled by plasmonic nanoantennas, including solar energy harvesting,^[76] infrared absorbers for thermal detectors,^[77] wireless on-chip communications,^[78] as well as optical microscopy, spectroscopy, and sensing.^[79]

Despite the relevant differences between RF and optical frequency ranges, the theoretical background and antenna con-

cepts established at RF can be at least partially applied to the design and modeling of optical nanoantennas. The concept of optical impedance of a plasmonic nanoantenna, also developed within the framework of optical nanocircuit theory, has proved to be especially useful in this context. Indeed, the notion of input impedance introduced in the first half of the 20th century^[80] allowed modularizing a physical antenna as a circuit load, characterized by its own impedance and terminals seen from the feeding line, avoiding the need of solving complicated integral equations every time the antenna was connected to a physical system. In a similar fashion, the design and operation of a plasmonic nanoantenna can be greatly simplified by the concept of optical impedance, which allows tuning and matching the nanoantenna in analogy to an RF radiator, without solving the full-wave electromagnetic problem every time.

Consider a linear dipole antenna, formed by two linear arms separated by a small gap (Figs. 4(a) and 4(b)). Its radiation/scattering properties and frequency response can be systematically optimized and tuned by using proper “loading” techniques,^[81] as routinely done by RF and microwave engineers. As depicted in Fig. 4(a), (left) a linear RF antenna is loaded at its gap with lumped circuit elements that, by changing the antenna input impedance, allow to operate at a given frequency or to achieve a good match to a specific feeding network, without the need of modifying the antenna’s physical properties, such as its length. Optical nanocircuits open the same possibilities for optical nanoantennas (Fig. 4(a), right), fully translating the systematic design methodologies of conventional low-frequency radiators. The complex optical input impedance of the nanoantenna, $Z_{in} = R_{in} - iX_{in}$, is defined, within the framework of optical nanocircuit theory, as the ratio of the applied voltage at the gap and the induced flux of displacement current across the dipole terminals (R_{in} and X_{in} represent, respectively, the antenna input resistance and reactance). As sketched in the inset of Fig. 4(a), this input impedance can be interpreted as the parallel combination of the dipole intrinsic impedance Z_{dip} and the gap impedance Z_{gap} .^[64,82] While the former is assumed to be a fixed property of the nanoantenna geometry and surrounding environment, the latter can be engineered to a large extent by loading the gap with different materials. For a cylindrical gap of height t , radius a and permittivity ϵ , excited by an electric field parallel to its axis, the gap impedance is given by^[64]

$$Z_{gap} = \frac{it}{\omega\epsilon\epsilon_0\pi a^2}, \quad (7)$$

which is inductive (capacitive), for negative (positive) values of $\text{Re}[\epsilon]$. Therefore, by filling the gap with dielectric or plasmonic materials (or their proper series or parallel combination^[63,64]), the input impedance of the nanoantenna

can be tailored to a large degree, based on this intuitive and elegant nanocircuit model. In analogy with RF radiators, it is possible to tune the resonance of the nanoantenna at the desired frequency ω_0 by properly designing the nanoload such that the overall reactance is compensated, i.e., $\text{Im}[Z_{\text{gap}}(\omega_0)] = -\text{Im}[Z_{\text{dip}}(\omega_0)]$ (Fig. 4(b)). Besides, based on the same concepts, we can also fully control the nanoantenna input resistance at resonance, which determines the impedance matching of the nanoantenna to a given feeding system,^[78] such as an optical transmission line or a quantum dot, maximizing the power delivered to the far-field from nanoscale sources, and *vice versa*.

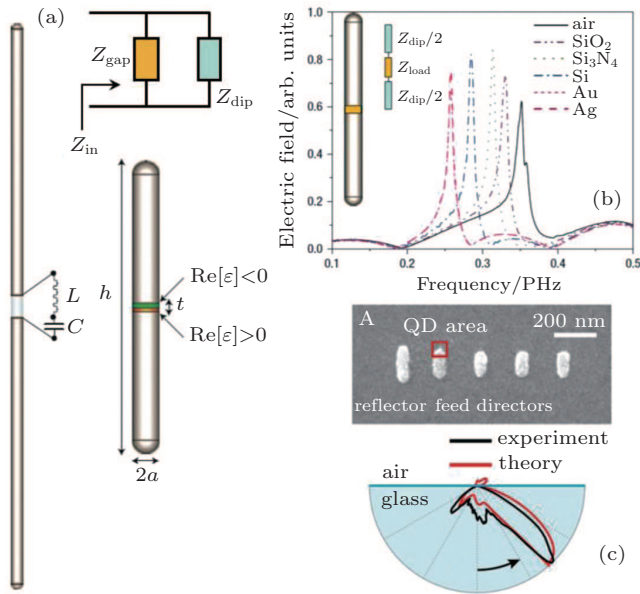


Fig. 4. Optical nanoantennas. (a) RF dipole antenna (left) loaded with lumped circuit elements at its feeding gap and, analogously, a plasmonic dipole nanoantenna (right) loaded with optical nanocircuits (from Ref. [64], Fig. 1). The top inset shows the circuit model of the antenna input impedance. (b) Tuning of the nanoantenna resonance by “gap loading” with different realistic materials (from Ref. [64], Fig. 3). (c) Example of advanced optical nanoantenna: Yagi-Uda nanoarray (SEM image) driven by a quantum dot, exhibiting a highly-directional radiation pattern (bottom panel) (from Ref. [86], Figs. 1(a) and 2(c)).

Nanoantennas composed of a single nanoparticle or paired elements (e.g., nanodimers,^[83] nanobowties^[84]) are electrically small and, therefore, exhibit a weakly directive radiation pattern (with directivity of about 1.76 dB, typical of small dipole antennas^[81]) and a dominant electric dipole response. In order to increase the directivity of the emitted radiation and design a more interesting scattering response, collections of several closely-spaced nanoparticles can be considered. As we discussed in Section 2, clusters and rings of plasmonic nanoparticles can be designed to tailor the flow of displacement current, supporting higher-order multipolar scattering patterns and tailored interference between plasmonic modes. This results in a more interesting temporal and spatial response of plasmonic nanoantennas, with moderately directive radiation patterns and sharper scattering resonances. A

particularly interesting example of optical nanoantenna is the Yagi-Uda array configuration in Fig. 4(c).^[56,85,86] Drawing inspiration from its popular RF counterpart, the design consists of a nanoantenna element driven by a localized optical source (e.g., a quantum dot), whose radiation is then directed and shaped by the neighboring parasitic nanoelements. The resulting radiation pattern has much higher directivity compared to individual nanoantennas, particularly appealing for enhanced radiation from single-photon quantum sources,^[86] with potential for narrow-angle beam steering of nanoscale optical emission. Finally, very large arrays of nanoantennas are particularly well-suited to realize three-dimensional (3D) metamaterials and two-dimensional (2D) metasurfaces, as their very short resonance length^[87] is ideal to achieve strong resonant optical response at the nanoscale, while keeping a deeply subwavelength separation between neighboring elements. The very small array period prevents the onset of grating lobes, realizing a locally homogenous effective response that enables anomalous optical effects, as further discussed in the next section.

4. Metasurfaces and flatland nanophotonics

Two-dimensional arrays of plasmonic nanoantennas are at the basis of optical metasurfaces — the planarized version of metamaterials — which strongly interact with the incident light over their subwavelength thickness, enabling new and distinctive phenomena and functionalities. Metasurfaces relax many of the limitations and drawbacks typically associated with 3D metamaterials, especially their high sensitiveness to ohmic losses and the challenges of fabricating 3D arrays at optical frequencies, which have typically limited the complete development of metamaterial technology. For these reasons, metasurfaces are often indicated as one of the most promising future directions in the field of optical metamaterials,^[88] as their reduced dimensionality provides the possibility to fully control light on planar ultra-thin platforms, realizing a new paradigm of “flatland nanophotonics”.

In this context, the recent demonstration of “generalized Snell’s laws of refraction” over an ultrathin metasurface in Ref. [89] triggered a lot of attention in the scientific community. The idea is based on imparting transverse phase discontinuities on a beam propagating through an inhomogeneous array of V-shaped plasmonic nanoantennas (Fig. 5). By spatially varying the shape and orientation of the nanoelements on the metasurface, the desired transverse phase pattern is achieved, opening the exciting possibility of controlling and molding the optical transmission and reflection at the nanoscale. For example, a metasurface formed by a periodically repeated supercell, as in Fig. 5(a), can be designed to realize a constant phase gradient that, by providing an additional transverse momentum, bends the transmitted beam at the desired angle, a response

similar to blazed gratings optimized for a specific diffraction order, but on an ultrathin platform. In general, the arrangement of nanoantennas does not need to be periodic, as the anomalous reflection and refraction properties are based on the local scattering response of the nanoantennas, rather than on collective behaviors.^[89] These planar arrays of nanoantennas have indeed provided great flexibility in the design of interesting optical effects, including anomalous reflection and refraction,^[89,90] generation of vortex beam carrying orbital angular momentum with different topological charge,^[89] focusing with aberration-free flat lenses^[91] and holography.^[92] All these examples, however, have pointed out relevant limitations that may hinder the practical applicability of this technology. These metasurfaces, in fact, interact with only a limited fraction of the impinging energy (in the order of few percents) and the rest of the energy is lost in unwanted reflection and diffraction. Besides, anomalous effects are obtained for the cross-polarized component of the scattered field (i.e., the component orthogonal to the incident field), which further limits the overall efficiency, as the cross-polarization coupling is generally low. It should be noted that such limitations are not specific of these particular designs, but they are rather associated with fundamental bounds for 2D geometries. In particular, the extremely small thickness of these metasurfaces, which is considered their main advantage and point of strength, is actually a key limitation for their overall efficiency. Intuitively, it may be evident that any electric current distribution induced over an infinitesimally-thin surface radiates with equal intensity on both sides due to symmetry, which already reduces the transmission efficiency by half.^[93] A detailed analysis developed in Ref. [66] (and supplementary material therein) reveals that, when a lossless, reciprocal and isotropic metasurface with zero thickness is illuminated by a linearly-polarized electromagnetic wave, power conservation and symmetry require the amplitude and phase of the transmission coefficient to be constrained by the relation: $|T| = \cos(\angle T)$. This implies that the maximum accessible phase range is limited to $[-\pi/2, \pi/2]$, with the transmission amplitude necessarily decreasing while approaching the extremes of this range. This explains why most metasurfaces to date^[89–92] have considered anisotropic nanoantenna elements operating with cross-polarized beams, which avoid this limitation at the expense of efficiency. Indeed, anisotropic metasurfaces can be described by a four-port network, for which the co-polarized T_{xx} and cross-polarized T_{xy} transmission coefficients satisfy the generalized condition^[66]

$$|T_{xx}|^2 - \text{Re}[T_{xx}] + |T_{xy}|^2 = 0. \quad (8)$$

Now the phase of T_{xy} can in principle span the entire range of transmission phases, allowing to impart an arbitrary phase pattern to the impinging wave; however, the previous equation

also proves that the theoretical maximum cross-coupling obtainable with an ultrathin metasurface is $|T_{xy}|^2 = 0.25$. Given the generality of these stringent limitations, it is clear that simple optimization of the nanoantenna inclusions in Ref. [89] is not sufficient, and novel designs and geometries need instead to be used in order to improve the performance.

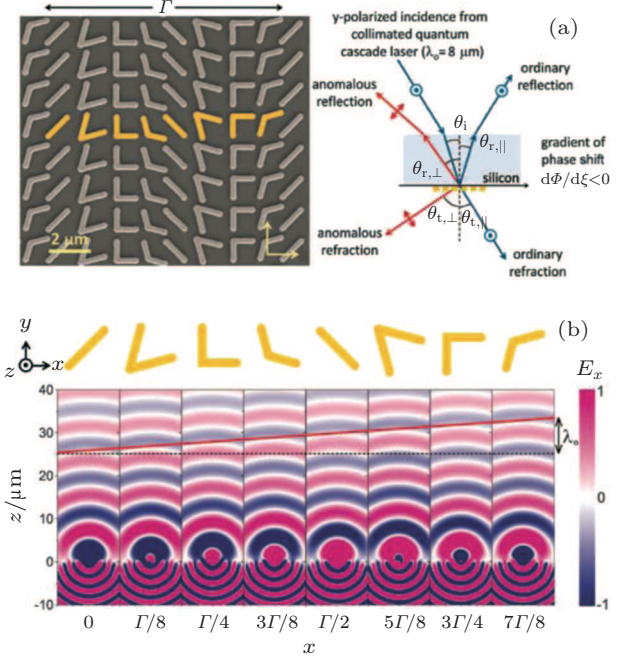


Fig. 5. Ultra-thin metasurfaces based on V-shaped nanoantennas. (a) 2D array of plasmonic nanoantennas, with the periodically-repeated supercell highlighted in yellow. As shown in the full-wave simulations in panel (b), this set of nanoantennas provides full phase control of the cross-polarized scattered field, enabling anomalous reflection and refraction properties (from Ref. [89], Figs. 2(f)–2(g) and 3(a)–3(b)).

The above limitations can be relaxed with metasurfaces operating in reflection mode, in which 100% reflection efficiency may be achieved by placing a highly reflective layer behind the metasurface, while maintaining full control of the phase.^[94,95] Nevertheless, operation in transmission may offer fundamental advantages in many practical cases and, therefore, it is worth investigating how to improve their performance. The previous discussion suggests that, in the transmission scenario, it is possible to overcome the limitations by breaking the inherent longitudinal symmetries of ultrathin metasurfaces, “unbalancing” the scattering response in the forward and backward directions. A solution in this sense has been recently proposed in Refs. [96] and [97], which exploits both electric and magnetic currents induced on a metasurface to fully manipulate the transmitted wavefront, based on electromagnetic equivalence principles.^[81] The transverse magnetic currents, supported by a small, yet finite, thickness, radiate anti-symmetric fields on the two sides of the metasurface, hence avoiding the radiation symmetry and overcoming the bounds defined by Eq. (8). Based on these principles, magneto–electric metasurfaces can indeed fully manip-

ulate the co-polarized transmitted beam with very high efficiency and minimized reflection.^[96,97] The need of exciting a strong transverse magnetic response makes this metasurface design well-suited for applications at low frequencies, RF and microwaves, where it is easy to realize magnetic inclusions, such as split-ring resonators; instead, this is particularly challenging at optical frequencies since the magnetic response is typically weak, as we discussed in Section 2. A solution specifically tailored for the optical frequency range has been proposed in Ref. [66], based on a symmetric stack of three only-electric metasurfaces, which has been shown to be the simplest non-magnetic structure able to fully control the transmitted beam, while ensuring zero reflection, i.e., impedance-matching to free-space. Again, the radiation symmetry is broken by a finite longitudinal thickness. Taking inspiration from RF transmitarrays,^[98] the metasurfaces are locally modeled as shunt reactances separated by transmission-line segments and, by solving this transmission-line model for a desired transmission phase pattern, the required profiles of the surface reactances can be found in closed-form.^[66] These impedance profiles can then be synthesized as realistic structures at optical frequencies thanks to optical nanocircuit theory, which proves once more to be a fundamental design tool for nanophotonics structures.^[99] The fundamental building block is formed by paired plasmonic and dielectric nanorods, realizing an inductor–capacitor nanocircuit (Fig. 6(a), left) whose impedance depends directly on the filling ratio of plasmonic and dielectric materials.^[66] By suitably alternating these nanocircuit blocks on the transverse direction, we can synthesize a metasurface with the desired inhomogeneous impedance profile. The resulting “meta-transmitarray”, composed of a stack of three metasurfaces (Fig. 6(a), right), can fully control the nanoscale optical transmission, while simultaneously minimizing the reflection, allowing, for example, light deflection with almost ideal efficiency as shown in Fig. 6(b). Extension to full manipulation of the transmission amplitude, in addition to the phase, can also be readily envisioned by adding engineered ohmic losses in the design (e.g., with resistive sheets), or by introducing properly tailored polarization cross-coupling, which would be seen as localized loss by the polarization of interest.

If it is possible to manipulate the near-field amplitude and phase on the metasurface with nanoscale precision, it is also possible to imprint an arbitrary operation to the metasurface transfer function. Recent theoretical explorations in this context^[100] have shown that it is in principle possible to arrange the modular nanoblocks on a metasurface to imprint the desired Green’s function to the output, and therefore apply any linear operation of choice to the impinging beam. As the wave propagates across the composite screen and emerges at its output, the operation gets applied to the impinging beam, realiz-

ing an all-optical, very efficient, ultrafast analog computation.

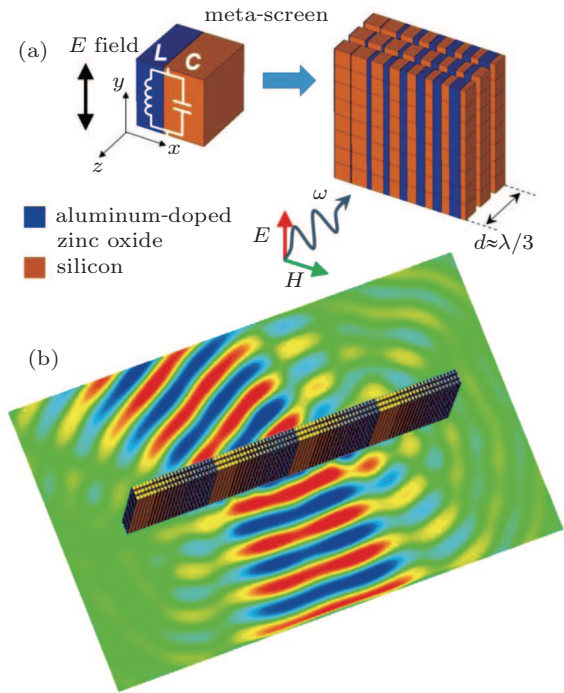


Fig. 6. Meta-transmitarray for full control of the nanoscale optical transmission. (a) Basic nanocircuit building block (left) and resulting meta-screen (right) with transverse inhomogeneous profiles of the surface impedance (from Ref. [99]). (b) Meta-transmitarray for light deflection with high efficiency and minimized reflections.^[66,99]

In addition to the exciting possibilities described in the previous paragraphs, advanced metasurfaces and meta-screens can also be designed to manipulate light absorption and emission (see, e.g., Ref. [101]), as well as to fully control the polarization state of propagating beams. Equation (8) shows that an infinitesimally-thin metasurface illuminated by a linearly-polarized wave cannot perform a perfect linear polarization conversion, namely, rotating a linear polarization state into its orthogonal one, since if the co-polarized transmission T_{xx} is zero, also the cross-polarized T_{xy} component must vanish. Again, to overcome these limitations, a thin meta-structure composed of three stacked metasurfaces has been recently proposed (Fig. 7(a)),^[102] which indeed realizes efficient and broadband linear polarization conversion. Moreover, 2D arrays of suitably designed nanoantennas have been put forward to realize broadband ultrathin quarter-wave plates;^[103] and multilayered “twisted metasurfaces”,^[104] obtained by imparting a sequential rotation to stacked nanoantenna arrays (Fig. 7(b)), have been shown to provide strong chiral response, allowing the realization of ultrathin broadband circular polarizers. The circular-polarization properties of light (photon spin angular momentum) are also related to the physics of geometrical Pancharatnam–Berry phase (see, e.g., Refs. [105] and [106]), which is at the basis of a number of planar optical elements, including flat blazed diffraction gratings and polarization-dependent focusing lenses.^[105] In this context, plasmonic metasurfaces can also be used to enhance photon

spin-orbit interactions,^[106] allowing to observe weak fundamental phenomena such as the photonic spin Hall effect.^[107]

Recent important trends in metasurface research include the realization of large-area flexible structures^[108,109] and the introduction of tunability and reconfigurability by integrating

the metasurfaces with tunable materials, such as graphene^[110] or transparent conducting oxides.^[111] These advances hold the promise to enable a full control of the state of light and realize system-level functionalities based on thin plasmonic metasurface platforms.

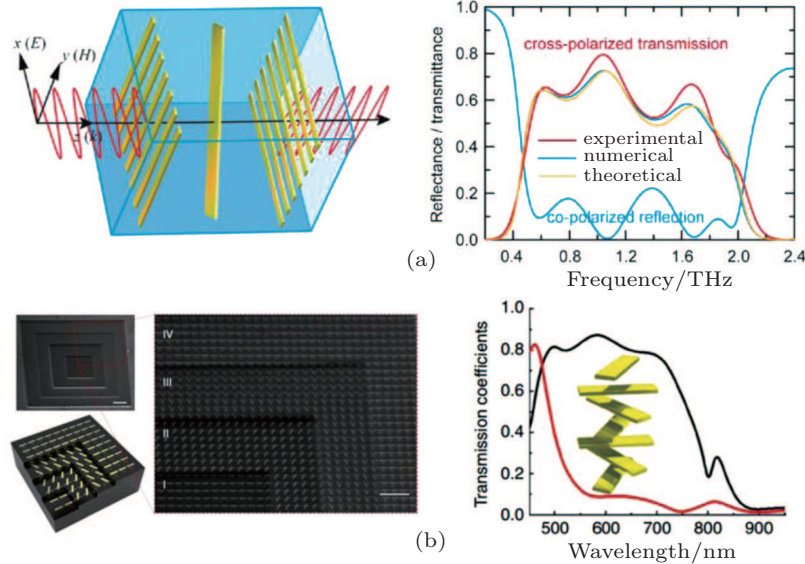


Fig. 7. Multilayered metasurfaces for controlling the polarization state of light. (a) Broadband linear polarization converter based on three stacked metasurfaces (unit cell shown in the left panel) (from Ref. [102], Figs. 2(a)–2(b)). (b) “Twisted metasurfaces” providing strong chiral response, which can be exploited to realize broadband ultrathin circular polarizers (from Ref. [104], Figs. 2(f) and 4(b)).

5. Conclusions and outlook

In this review paper, we have discussed some of the most exciting and promising research directions in the field of plasmonic metamaterials. As we move upward in the “design stack”, from the “physical layer” of plasmonic nanoparticles and nanoclusters, to more complex plasmonic components and devices, like nanoantennas and metasurfaces, new emergent phenomena and more complex functionalities may be synthesized at each level, paving the way to a new era for nanophotonics. Modularization concepts, like the toolbox of optical nanocircuit theory, allow interfacing the different levels and building simple and effective designs from an underlying physical richness and complexity. Thanks to the notion of optical nanocircuits, we can also borrow and translate relevant knowledge from other well-established fields, notably, electrical circuit theory and microwave engineering, greatly simplifying the design of, for example, plasmonic nanoantennas in analogy with their RF counterparts. Particular attention deserves the subfield of plasmonic metasurfaces, which aims at providing a system-level platform for the full control of light (amplitude, phase, frequency, spin, and orbital angular momentum), up to the single-photon level, combined with the possibility of integration in reconfigurable systems. For example, these concepts may pave the way to the realization of large-area, flexible, ultrafast spatial light modulators with subwavelength thickness and nanoscale resolution, materializ-

ing some of the early promises of nanotechnology in the field of optics.^[112] For all these reasons, we feel confident that the metamaterial revolution at the nanoscale has just started, and will present exciting new developments in the realm of practical applications in the coming years.

References

- [1] Engheta N and Ziolkowski R 2006 *Electromagnetic Metamaterials: Physics and Engineering Explorations* (Hoboken, NJ: Wiley-IEEE Press)
- [2] Engheta N 2002 *International Conference on Mathematical Methods in Electromagnetic Theory* **1** 175
- [3] Sihvola A 2007 *Metamaterials* **1** 2
- [4] Shelby R A, Smith D R and Schultz S 2001 *Science* **292** 77
- [5] Veselago V G 1968 *Sov. Phys. Uspekhi* **10** 509
- [6] Pendry J B 2000 *Phys. Rev. Lett.* **85** 3966
- [7] Born M and Wolf E 2002 *Principles of Optics: Electromagnetic Theory of Propagation, Interference and Diffraction of Light* (Cambridge: Cambridge University Press)
- [8] Alù A and Engheta N 2005 *Phys. Rev. E* **72** 16623
- [9] Pendry J B, Schurig D and Smith D R 2006 *Science* **312** 1780
- [10] Rainwater D, Kerkhoff A, Melin K, Soric J C, Moreno G and Alù A 2012 *New J. Phys.* **14** 013054
- [11] Schurig D, Mock J J, Justice B J, Cummer S A, Pendry J B, Starr A F and Smith D R 2006 *Science* **314** 977
- [12] Alù A 2009 *Phys. Rev. B* **80** 245115
- [13] Tretyakov S, Alitalo P, Luukkonen O and Simovski C 2009 *Phys. Rev. Lett.* **103** 103905
- [14] Leonhardt U and Philbin T G 2006 *New J. Phys.* **8** 247
- [15] Narimanov E E and Kildishev A V 2009 *Appl. Phys. Lett.* **95** 041106
- [16] Smolyaninov I I 2011 *Phys. Rev. Lett.* **107** 253903
- [17] Smolyaninov I I and Smolyaninova V N 2013 Is there a metamaterial route to high temperature superconductivity? arXiv: 1311.3277v2 [physics.optics]

- [18] Joannopoulos J D, Johnson S G, Winn J N and Meade R D 2008 *Photonic Crystals: Molding the Flow of Light*, 2nd edn. (NJ: Princeton University Press)
- [19] Sihvola A 1999 *Electromagnetic Mixing Formulas and Applications* (London: IEEE Press)
- [20] Tretyakov S 2002 *Analytical Modeling in Applied Electromagnetics* (Norwood: Artech House)
- [21] Alù A 2011 *Phys. Rev. B* **84** 075153
- [22] Maier S A 2007 *Plasmonics: Fundamentals and Applications* (New York: Springer)
- [23] Bohren C F and Huffman D R 1983 *Absorption and Scattering of Light by Small Particles* (New York: Wiley)
- [24] Alù A and Engheta N 2005 *J. Appl. Phys.* **97** 094310
- [25] West J L and Halas N J 2003 *Ann. Rev. Biomed. Eng.* **5** 285
- [26] Anker J N, Hall W P, Lyandres O, Shah N C, Zhao J and Van Duyne R P 2008 *Nat. Mater.* **7** 442
- [27] Aubry A, Lei D Y, Fernández-Domínguez A I, Sonnefraud Y, Maier S A and Pendry J B 2010 *Nano Lett.* **10** 2574
- [28] Atwater H A and Polman A 2010 *Nat. Mater.* **9** 205
- [29] Willets K A and Van Duyne R P 2007 *Ann. Rev. Phys. Chem.* **58** 267
- [30] Argyropoulos C, Chen P Y, Monticone F, D'Aguanno G and Alù A 2012 *Phys. Rev. Lett.* **108** 263905
- [31] Alù A and Engheta N 2009 *Phys. Rev. Lett.* **102** 233901
- [32] Alù A and Engheta N 2010 *Phys. Rev. Lett.* **105** 263906
- [33] Kallos E, Argyropoulos C, Hao Y and Alù A 2011 *Phys. Rev. B* **84** 045102
- [34] Monticone F and Alù A 2013 *Phys. Rev. X* **3** 041005
- [35] Selvanayagam M and Eleftheriades G V 2013 *Phys. Rev. X* **3** 041011
- [36] Chen P Y, Argyropoulos C and Alù A 2013 *Phys. Rev. Lett.* **111** 233001
- [37] Alù A and Engheta N 2010 *J. Nanophotonics* **4** 041590
- [38] Sipe J and Kranendonk J 1974 *Phys. Rev. A* **9** 1806
- [39] Alù A and Engheta N 2008 *New J. Phys.* **10** 115036
- [40] Monticone F, Argyropoulos C and Alù A 2013 *Phys. Rev. Lett.* **110** 113901
- [41] Foster R M 1924 *Bell Syst. Tech. J.* **3** 259
- [42] Argyropoulos C, Monticone F, D'Aguanno G and Alù A 2013 *Appl. Phys. Lett.* **103** 143113
- [43] Monticone F, Argyropoulos C and Alù A 2012 *Sci. Rep.* **2** 912
- [44] Mackowski D W 1994 *J. Opt. Soc. Am. A* **11** 2851
- [45] Prodan E, Radloff C, Halas N J and Nordlander P 2003 *Science* **302** 419
- [46] Nordlander P, Oubre C, Prodan E, Li K and Stockman M I 2004 *Nano Lett.* **4** 899
- [47] Alù A and Engheta N 2008 *Phys. Rev. B* **78** 085112
- [48] Luk'yanchuk B, Zheludev N I, Maier S A, Halas N J, Nordlander P, Giessen H and Chong C T 2010 *Nat. Mater.* **9** 707
- [49] Miroshnichenko A E, Flach S and Kivshar Y S 2010 *Rev. Mod. Phys.* **82** 2257
- [50] Lassiter J B, Sobhani H, Fan J A, Kundu J, Capasso F, Nordlander P and Halas N J 2010 *Nano Lett.* **10** 3184
- [51] Wu C, Khanikaev A B, Adato R, Arju N, Yanik A A, Altug H and Shvets G 2012 *Nat. Mater.* **11** 69
- [52] Alù A, Salandrino A and Engheta N 2006 *Opt. Express* **14** 1557
- [53] Landau L D, Pitaevskii L P and Lifshitz E M 1984 *Electrodynamics of Continuous Media* (Oxford: Butterworth-Heinemann)
- [54] Fan J A, Wu C, Bao K, Bao J, Bardhan R, Halas N J, Manoharan V N, Nordlander P, Shvets G and Capasso F 2010 *Science* **328** 1135
- [55] Shafiei F, Monticone F, Le K Q, Liu X X, Hartsfield T, Alù A and Li X 2013 *Nat. Nanotechnol.* **8** 95
- [56] Engheta N 2007 *Science* **317** 1698
- [57] Brongersma M L and Shalaev V M 2010 *Science* **328** 440
- [58] Engheta N, Salandrino A and Alù A 2005 *Phys. Rev. Lett.* **95** 095504
- [59] Alù A and Engheta N 2011 *Proc. IEEE* **99** 1669
- [60] Pozar D M 2011 *Microwave Engineering*, 3rd edn. (New York: Wiley)
- [61] Sun Y, Edwards B, Alù A and Engheta N 2012 *Nat. Mater.* **11** 208
- [62] Shi J, Elias S, Monticone F, Wu Y, Ratchford D, Li X and Alù A 2014 Modular Assembly of Optical Nanocircuits *under review*, 2014
- [63] Liu N, Wen F, Zhao Y, Wang Y, Nordlander P, Halas N J and Alù A 2013 *Nano Lett.* **13** 142
- [64] Alù A and Engheta N 2008 *Nat. Photonics* **2** 307
- [65] Brongersma M L 2008 *Nat. Photonics* **2** 270
- [66] Monticone F, Estakhri N M and Alù A 2013 *Phys. Rev. Lett.* **110** 203903
- [67] Walther C, Scalari G, Amanti M I, Beck M and Faist J 2010 *Science* **327** 1495
- [68] Alù A and Engheta N 2009 *Phys. Rev. Lett.* **103** 143902
- [69] Agio M and Alù A 2013 *Optical Antennas* (New York: Cambridge University Press)
- [70] Palomba S, Danckwerts M and Novotny L 2009 *J. Opt. A: Pure Appl. Opt.* **11** 114030
- [71] Chen P Y and Alù A 2010 *Phys. Rev. B* **82** 235405
- [72] Chen P Y, Argyropoulos C and Alù A 2012 *Nanophotonics* **1** 221
- [73] Greffet J J 2005 *Science* **308** 1561
- [74] Mühlischlegel P, Eisler H J, Martin O J F, Hecht B and Pohl D W 2005 *Science* **308** 1607
- [75] Akimov A V, Mukherjee A, Yu C L, Chang D E, Zibrov A S, Hemmer P R, Park H and Lukin M D 2007 *Nature* **450** 402
- [76] Cao L, Fan P, Vasudev A P, White J S, Yu Z, Cai W, Schuller J A, Fan S and Brongersma M L 2010 *Nano Lett.* **10** 439
- [77] Zhu H, Yi F and Cubukcu E 2012 *IEEE Photonics Technol. Lett.* **24** 1194
- [78] Alù A and Engheta N 2010 *Phys. Rev. Lett.* **104** 213902
- [79] Biagioni P, Huang J S and Hecht B 2012 *Rep. Prog. Phys.* **75** 024402
- [80] Oliner A A 1984 *IEEE Trans. Microw. Theory Tech.* **32** 1022
- [81] Balanis C A 2005 *Antenna Theory: Analysis and Design* (New York: Wiley)
- [82] Alù A and Engheta N 2008 *Phys. Rev. Lett.* **101** 043901
- [83] Alù A and Engheta N 2008 *Phys. Rev. B* **78** 195111
- [84] Schuck P J, Fromm D P, Sundaramurthy A, Kino G S and Moerner W E 2005 *Phys. Rev. Lett.* **94** 017402
- [85] Li J, Salandrino A and Engheta N 2007 *Phys. Rev. B* **76** 245403
- [86] Curto A G, Volpe G, Taminiau T H, Kreuzer M P, Quidant R and van Hulst N F 2010 *Science* **329** 930
- [87] Novotny L 2007 *Phys. Rev. Lett.* **98** 266802
- [88] Kildishev A V, Boltasseva A and Shalaev V M 2013 *Science* **339** 1232009
- [89] Yu N, Genevet P, Kats M A, Aieta F, Tetienne J P, Capasso F and Gaburro Z 2011 *Science* **334** 333
- [90] Ni X, Emani N K, Kildishev A V, Boltasseva A and Shalaev V M 2012 *Science* **335** 427
- [91] Aieta F, Genevet P, Kats M A, Yu N, Blanchard R, Gaburro Z and Capasso F 2012 *Nano Lett.* **12** 4932
- [92] Ni X, Kildishev A V and Shalaev V M 2013 *Nat. Commun.* **4** 2807
- [93] Alù A 2013 *Physics* **6** 53
- [94] Pors A, Albrektsen O, Radko I P and Bozhevolnyi S I 2013 *Sci. Rep.* **3** 2155
- [95] Sun S, He Q, Xiao S, Xu Q, Li X and Zhou L 2012 *Nat. Mater.* **11** 426
- [96] Pfeiffer C and Grbic A 2013 *Phys. Rev. Lett.* **110** 197401
- [97] Selvanayagam M and Eleftheriades G V 2013 *Opt. Express* **21** 14409
- [98] Pozar D M 1996 *Electron. Lett.* **32** 2109
- [99] Monticone F and Alù A 2013 *OPN-Year in Optics* **24** 35
- [100] Silva A, Monticone F, Castaldi G, Galdi V, Alù A and Engheta N 2014 *Science* **343** 160
- [101] Argyropoulos C, Le K Q, Mattiucci N, D'Aguanno G and Alù A 2013 *Phys. Rev. B* **87** 205112
- [102] Grady N K, Heyes J E, Chowdhury D R, Zeng Y, Reiten M T, Azad A K, Taylor A J, Dalvit D A R and Chen H T 2013 *Science* **340** 1304
- [103] Zhao Y and Alù A 2013 *Nano Lett.* **13** 1086
- [104] Zhao Y, Belkin M A and Alù A 2012 *Nat. Commun.* **3** 870
- [105] Hasman E, Kleiner V, Biener G and Niv A 2003 *Appl. Phys. Lett.* **82** 328
- [106] Bliokh K Y, Niv A, Kleiner V and Hasman E 2008 *Nat. Photonics* **2** 748
- [107] Yin X, Ye Z, Rho J, Wang Y and Zhang X 2013 *Science* **339** 1405
- [108] Chanda D, Shigeta K, Gupta S, Cain T, Carlson A, Mihi A, Baca A J, Bogart G R, Braun P and Rogers J A 2011 *Nat. Nanotechnol.* **6** 402
- [109] Li P C and Yu E T 2013 *J. Appl. Phys.* **114** 133104
- [110] Mousavi S H, Kholmanov I, Alici K B, Purtseladze D, Arju N, Tatar K, Fozdar D Y, Suk J W, Hao Y, Khanikaev A B, Ruoff R S and Shvets G 2013 *Nano Lett.* **13** 1111
- [111] Fleischer K, Arca E, Smith C and Shvets I V 2012 *Appl. Phys. Lett.* **101** 121918
- [112] Wowk B 1996 "Phased Array Optics", in *Nanotechnology: Molecular Speculations on Global Abundance* (Cambridge: MIT Press)